



Inter-Vendor Reproducibility of Pseudo-Continuous Arterial Spin Labeling at 3 Tesla

Henri J. M. M. Mutsaerts^{1*}, Rebecca M. E. Steketee², Dennis F. R. Heijtel¹, Joost P. A. Kuijjer³, Matthias J. P. van Osch⁴, Charles B. L. M. Majoie¹, Marion Smits², Aart J. Nederveen¹

1 Department of Radiology, Academic Medical Center, Amsterdam, The Netherlands, **2** Department of Radiology, Erasmus MC University Medical Center Rotterdam, Rotterdam, The Netherlands, **3** Department of Physics and Medical Technology, VU University Medical Center, Amsterdam, The Netherlands, **4** C. J. Gorter Center for High Field MRI, Department of Radiology, Leiden University Medical Center, Leiden, The Netherlands

Abstract

Purpose: Prior to the implementation of arterial spin labeling (ASL) in clinical multi-center studies, it is important to establish its status quo inter-vendor reproducibility. This study evaluates and compares the intra- and inter-vendor reproducibility of pseudo-continuous ASL (pCASL) as clinically implemented by GE and Philips.

Material and Methods: 22 healthy volunteers were scanned twice on both a 3T GE and a 3T Philips scanner. The main difference in implementation between the vendors was the readout module: spiral 3D fast spin echo vs. 2D gradient-echo echo-planar imaging respectively. Mean and variation of cerebral blood flow (CBF) were compared for the total gray matter (GM) and white matter (WM), and on a voxel-level.

Results: Whereas the mean GM CBF of both vendors was almost equal ($p=1.0$), the mean WM CBF was significantly different ($p<0.01$). The inter-vendor GM variation did not differ from the intra-vendor GM variation ($p=0.3$ and $p=0.5$ for GE and Philips respectively). Spatial inter-vendor CBF and variation differences were observed in several GM regions and in the WM.

Conclusion: These results show that total GM CBF-values can be exchanged between vendors. For the inter-vendor comparison of GM regions or WM, these results encourage further standardization of ASL implementation among vendors.

Citation: Mutsaerts HJMM, Steketee RME, Heijtel DFR, Kuijjer JPA, van Osch MJP, et al. (2014) Inter-Vendor Reproducibility of Pseudo-Continuous Arterial Spin Labeling at 3 Tesla. PLoS ONE 9(8): e104108. doi:10.1371/journal.pone.0104108

Editor: Bart Rypma, University of Texas at Dallas, United States of America

Received: February 20, 2014; **Accepted:** July 8, 2014; **Published:** August 4, 2014

Copyright: © 2014 Mutsaerts et al. This is an open-access article distributed under the terms of the Creative Commons Attribution License, which permits unrestricted use, distribution, and reproduction in any medium, provided the original author and source are credited.

Funding: This work was financially supported by the Dutch non-governmental organizations Stichting Coolsingel (grant 179) and NutsOhra (grant 1002-031). The funders had no role in study design, data collection and analysis, decision to publish, or preparation of the manuscript.

Competing Interests: The authors have declared that no competing interests exist.

* Email: henkjanmutsaerts@gmail.com

Introduction

Arterial spin labeling (ASL) is an emerging magnetic resonance imaging (MRI) perfusion modality that enables non-invasive cerebral perfusion measurements. Since ASL is virtually harmless, not hampered by the blood-brain barrier and enables absolute quantification of cerebral blood flow (CBF), it is an attractive tool compared to other perfusion imaging modalities [1,2]. Through several methodological advances, ASL perfusion MRI has matured to the point where it can provide high quality whole-brain perfusion images in only a few minutes of scanning [3]. Its reproducibility has been established and its CBF-maps are comparable with imaging methods based on exogenous tracers [4–7]. ASL is commercially available on all major MRI systems and clinical applications are under rapid development. ASL-based CBF measurements are of clinical value in a number of cerebral pathologies, such as brain tumors, cerebrovascular pathology, epilepsy and neurodegeneration [8,9]. Therefore, the initiation of large-scale multi-center ASL studies is a next step to extend our understanding of the pathophysiology of many common disorders.

However, it is essential to first establish the inter-vendor reproducibility of ASL [10,11]. One main obstacle that impedes multi-center studies, is that fundamental differences exist between ASL implementations of different vendors. Each MRI vendor has implemented a different labeling-readout combination, which may seriously hamper the comparison of multi-vendor ASL-data [12]. Since each labeling and readout strategy exhibits specific advantages and disadvantages, a substantial technical heterogeneity is introduced [13]. Therefore, it remains unclear to which degree ASL-based CBF-maps from centers with scanners of different vendors are comparable. The aim of the current study is to assess and compare the intra- and inter-vendor reproducibility of pseudo-continuous ASL (pCASL) CBF measurements as currently clinically implemented by two major vendors: i.e. GE and Philips.

Materials and Methods

Subject recruitment and study design

Twenty-two healthy volunteers (9 men, 13 women, mean age 22.6 ± 2.1 (SD) years) were included. In addition to standard MRI

exclusion criteria, subjects with history of brain or psychiatric disease or use of medication - except for oral contraceptives - were excluded. No consumption of vasomotor substances such as alcohol, cigarettes, coffee, licorice and tea was allowed on the scan days. On the day prior to the examination, alcohol and nicotine consumption was restricted to three units and cigarettes respectively.

All subjects were scanned twice at two academic medical centers in the Netherlands: Erasmus MC – University Medical Center Rotterdam (center 1) and Academic Medical Center Amsterdam (center 2). The inter-session time interval was kept at 1–4 weeks. MRI experiments were performed on a 3T GE scanner at center 1 (Discovery MR750, GE Healthcare, Milwaukee, WI, US) and on a 3T Philips scanner at center 2 (Intera, Philips Healthcare, Best, the Netherlands), both equipped with an 8-channel head coil (InVivo, Gainesville, FL, US). Foam padding inside the head coil was used to restrict head motion during scanning [10]. Subjects were awake and had their eyes closed during all ASL scans.

Ethics statement

All subjects provided written informed consent and the study was approved by the ethical review boards of both centers.

Acquisition

Each scan session included a pCASL and 1 mm isotropic 3D T1-weighted scan for segmentation and registration purposes. For the acquisition of a single time-point CBF-map, pCASL has become the preferred labeling strategy because of its relatively high signal-to-noise ratio (SNR) and wide availability across all platforms [3,14]. On both scanners we employed the clinically implemented pCASL protocols that are currently used in clinical studies [15,16]. Table 1 and Figure 1 summarize the protocol details and show the timing diagrams for both sequences respectively. The main difference between the GE and Philips implementations was the readout module: multi-shot spiral 3D fast spin-echo vs. single-shot 2D gradient-echo echo-planar imaging respectively.

Post-processing: quantification

Matlab 7.12.0 (MathWorks, MA, USA) and Statistical Parametric Mapping (SPM) 8 (Wellcome Trust Center for Neuroimaging, University College London, UK) were used for post-processing and statistical analyses. For the Philips data, label and control pCASL images were pair-wise subtracted and averaged to obtain perfusion-weighted images. For the GE data, the perfusion-weighted images as directly provided by the scanner were used. Since the images as provided by GE did not incorporate motion correction, this was not applied to the Philips data. The perfusion-weighted maps of both vendors were quantified into CBF maps using a single compartment model [3,17]:

$$CBF(mL/100\text{ g}/\text{min}) = \frac{6000\Delta M e^{PLD/T_{1a}}}{2\alpha\alpha_{inv}M_{0a}T_{1a}(1 - e^{-\tau/T_{1a}})} \quad (1)$$

where ΔM represents the difference images between control and label and M_{0a} the equilibrium magnetization of arterial blood. In Philips, ΔM was corrected for the transversal magnetization decay time (T_2^*) of arterial blood (48 ms) during the 17 ms echo time (TE) by e^{TE/T_2^*} [18]. PLD is the post-labeling delay (1.525 s), T_{1a} is the longitudinal relaxation time of arterial blood (1.650 s), α is the labeling efficiency (0.8), where α_{inv} corrects for the decrease in labeling efficiency due to the 5 and 2 background suppression pulses at GE (0.75) and Philips (0.83) respectively and τ represents

the labeling duration (1.450 s and 1.650 s for GE and Philips respectively) [19–21]. The increase in label decay in the ascending acquired 2D slices in Philips-data was accounted for. GE has, but Philips has not, implemented a standard M_0 -acquisition where proton density maps are obtained with a saturation recovery acquisition using readout parameters identical to the ASL readout. These maps were converted to M_{0a} by the following equation:

$$M_{0a} = \frac{PD}{\lambda_{GM}(1 - e^{-\frac{t_{sat}}{T_{1GM}}})} \quad (2)$$

where t_{sat} is the saturation recovery time (2 s), T_{1GM} is the relaxation time of gray matter (GM) tissue (1.2 s) and λ_{GM} is the GM brain-blood water partition coefficient (0.9 mL/g) [15,22,23]. For the Philips data, a single M_{0a} -value was used for all subjects. This value was obtained in a previous study with the same center, scanner, head coil, pCASL protocol and a similar population ($n = 16$, 56% M, age 20–24 years) [24]. In short, cerebrospinal fluid T1 recovery curves were fitted on the control images of multiple time-point pCASL measurements, with the same readout, without background suppression. The acquired M_0 was converted to M_{0a} by multiplication with the blood water partition coefficient (0.76) and the density of brain tissue (1.05 g/mL) [23,25]. No difference was made between the quantification of GM and WM CBF.

Post-processing: spatial normalization

A single 3D T1-weighted anatomical scan from each scanner for each subject ($n = 44$) was segmented into GM and white matter (WM) tissue probability maps. All CBF maps were transformed into anatomical space by a rigid-body registration on the GM tissue probability maps. The tissue probability maps were spatially normalized using the Diffeomorphic Anatomical Registration analysis using Exponentiated Lie algebra (DARTEL) algorithm, and the resulting normalization fields were applied to the CBF maps as well [26]. Finally, all normalized images were spatially smoothed using an $8 \times 8 \times 8$ mm full-width-half-maximum Gaussian kernel, to minimize registration and interpolation errors.

Data analysis

All intra-vendor reproducibility analyses were based on a comparison of session 1 with session 2 within each vendor ($n = 22$). All inter-vendor reproducibility analyses were based on a comparison of GE session 1 with Philips session 2, and GE session 2 with Philips session 1 ($n = 44$). In this way, the temporal physiological variation is expected to have an equal contribution to the intra- and inter-vendor reproducibility. All reproducibility analyses were based on the mean CBF of the two sessions, and on the mean and standard deviation of the paired inter-session CBF difference, denoted as ΔCBF and $SD_{\Delta CBF}$ respectively. The within-subject coefficient of variation (wsCV) - a normalized parameter of variation - was defined as the ratio of $SD_{\Delta CBF}$ to the mean CBF of both sessions:

$$wsCV = 100\% \frac{SD_{\Delta CBF}}{meanCBF} \quad (3)$$

Reproducibility was assessed on a total GM and WM level, and on a voxel-level.

Table 1. Acquisition protocols.

	GE	Philips
Labeling module	pseudo-continuous	pseudo-continuous
Labeling pulse shape	Hanning	Hanning
Labeling pulse duration	0.5 ms	0.5 ms
Labeling pulse flip angle	23°	18°
Mean gradient strength	0.7 mT/m	0.6 mT/m
Maximal gradient strength	7 mT/m	6 mT/m
Labeling duration	1450 ms	1650 ms
Post-labeling delay (PLD) (initial)	1525 ms	1525 ms
PLD increase per slice	n.a.	28.3 ms
PLD (average)	1525 ms	1770 ms
Labeling plane planning	Fixed 22 mm below lower edge	89 mm below, parallel to AC-PC line
Labeling plane distance*	72 mm	89 mm
Readout module	3D fast spin-echo interleaved stack-of-spirals	2D gradient-echo single-shot echo-planar imaging SENSE 2.5, CLEAR
Acquisition matrix	8 spirals×512 sampling points	80×80
Field of view	24 cm ³	24 cm ²
Number of slices	36	17
Slice thickness	4 mm	7 mm
Acquisition voxel size (volume)	3.8×3.8×4 mm (57.8 mm ³)	3.0×3.0×7.0 mm (63 mm ³)
Reconstruction voxel size	1.9×1.9×4.0 mm	3.0×3.0×7.0 mm
Slice gap	n.a.	0 mm
Echo time/repetition time	10.5/4600 ms	17/4000 ms
Number of signal averages	3	33
Readout planning	True axial, lower edge fixed at lower boundary pons	Parallel to AC-PC line
Background suppression (n pulses)	yes (5)	yes (2)
Vascular crushing	no	no
Acquisition duration	4:29 min	4:33 min

*Labeling plane distance represents distance from the anterior commissure-posterior commissure (ACPC) line in the head-feet direction [20]. n.a. = not applicable.
doi:10.1371/journal.pone.0104108.t001

Data analysis: total supratentorial GM and WM

Mean CBF-values of each session were obtained for the total supratentorial GM and WM. GM and WM masks were obtained by thresholding GM and WM probability maps at 70% and 95% tissue probabilities respectively. GM-WM CBF ratios were calculated individually. The significance of paired inter-session CBF differences (Δ CBF) was tested with a paired two-tailed Student's t-test. The Levene's test was used to test the significance of the difference between GE $SD_{\Delta CBF}$ and Philips $SD_{\Delta CBF}$, as well as between the inter-vendor $SD_{\Delta CBF}$ and both intra-vendor $SD_{\Delta CBF}$ [27]. Limits of agreement - defining the range in which 95% of future measurements is expected to lie - were defined as $\Delta CBF \pm 1.96 SD_{\Delta CBF}$ [28].

Data analysis: voxel-level comparison

To assess spatial inter-vendor differences, CBF- and wsCV-values were computed for each voxel. For CBF, both sessions and all subjects were averaged. To test significant voxel-wise inter-vendor CBF differences, a Bonferroni-corrected paired two-tailed Student's t-test was performed (using both sessions, $n = 44$). Individual histograms of CBF (25 bins, range 0–160 mL/100 g/min) were averaged to generate a group-level histogram. A wsCV histogram (25 bins, range 5–45%) was generated from the wsCV-

maps. Both CBF and wsCV histograms were generated for the total supratentorial GM and WM of each vendor. Statistical significance was set to $p < 0.05$ for all tests.

Results

Session timing

The number of days between intra-vendor sessions did not differ between vendors: 18.3 ± 6.5 and 19.7 ± 7.2 for GE and Philips respectively (independent sample Student's t-test, $p = 0.5$). However, GE session 1 and session 2 took place earlier in the day compared to the Philips sessions ($15 \text{ h}26 \pm 4 \text{ h}00$ and $15 \text{ h}55 \pm 3 \text{ h}34$ compared to $20 \text{ h}16 \pm 2 \text{ h}06$ and $19 \text{ h}47 \pm 2 \text{ h}38$ respectively, $p < 0.01$).

Total GM and WM

The intra- and inter-vendor statistics are summarized in Table 2 and visualized by the Bland-Altman plots in Figure 2. GM CBF did not differ significantly between both vendors ($p = 1.0$), but WM CBF did ($p < 0.01$). Likewise, the intra-vendor GM variances of the paired CBF differences did not differ between the two vendors whereas the WM variances did ($p = 0.6$ and $p = 0.02$ respectively). The GM-WM CBF ratios of both vendors differed significantly, the 2D readout (Philips) GM-WM ratio

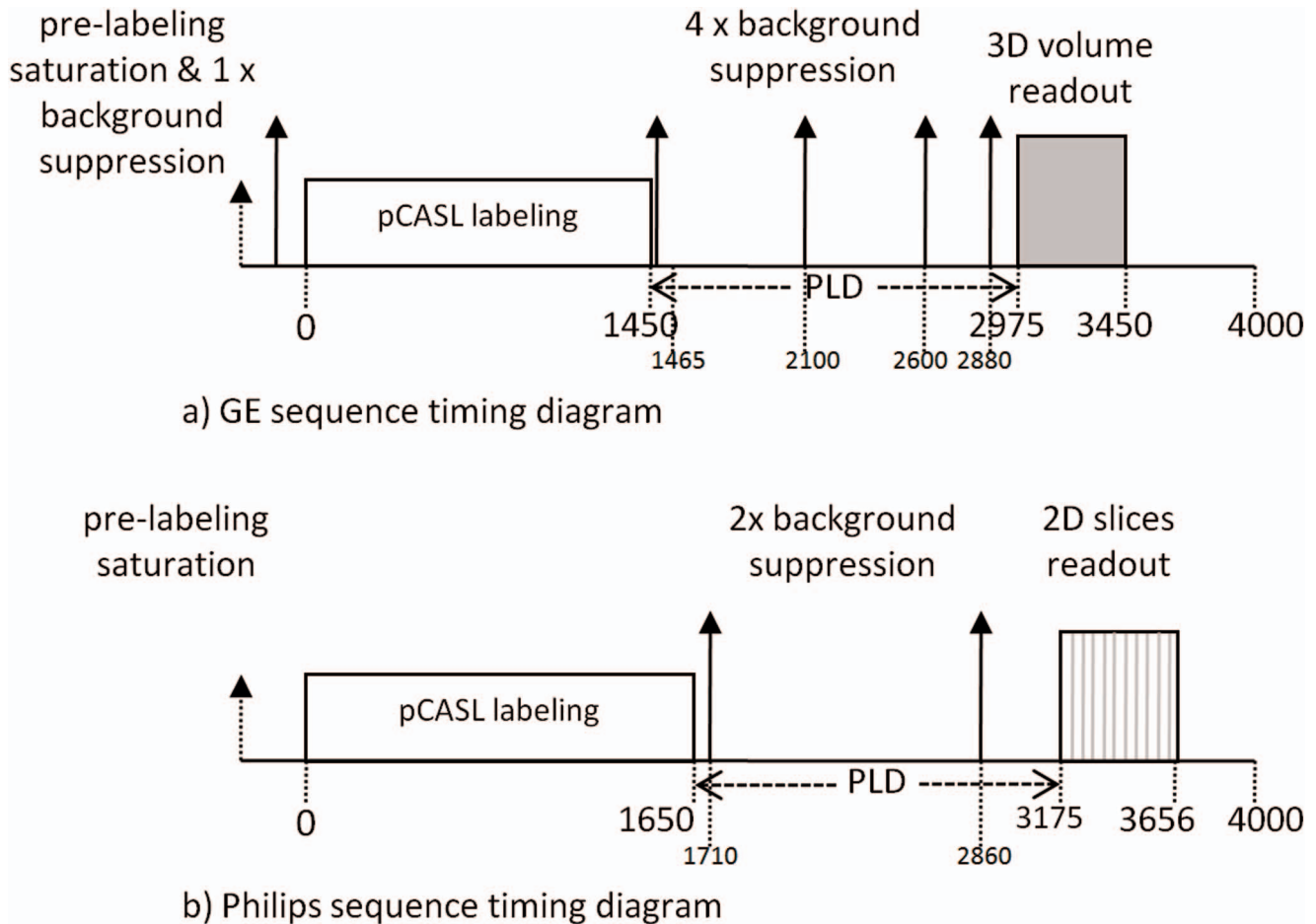


Figure 1. Sequence timing diagrams of a) General Electric (GE) and b) Philips, shown at the same time scale (ms). pCASL = pseudo-continuous arterial spin labeling, PLD = post-labeling delay.
doi:10.1371/journal.pone.0104108.g001

being approximately twice as large as the ratio of the 3D readout (GE) ($p < 0.01$). Both the GM and WM intra-vendor wsCVs were similar to the inter-vendor wsCVs (Table 2), which is confirmed by the Levene's test. The variance of GM inter-vendor CBF differences did not differ significantly from the variance of intra-vendor differences ($p = 0.3$ and $p = 0.5$ for GE and Philips respectively). For the WM, however, the variance of inter-vendor CBF differences did differ significantly from the Philips variance but not from the GE variance ($p = 0.02$ and $p = 0.8$ respectively).

Voxel-level comparison

Spatial CBF differences between GE and Philips are illustrated for a single subject and on group level in Figure 3 and 4 respectively. The spatial wsCV distribution is shown in Figure 5. In addition, Figure 6 provides an overview of spatial CBF differences between subjects, sessions and vendors for a single transversal slice. The main visual difference on all these maps was the homogeneity of GE compared to the heterogeneity of Philips, especially in the WM and in the z-direction. More specifically, the contrast between GM and WM was higher on the Philips CBF and wsCV-maps. Also within the GM, the CBF was more heterogeneous on the Philips maps compared to the GE maps. A CBF decrease and wsCV increase was observed in the posterior and superior regions on the GE maps and in the anterior-inferior and superior regions on the Philips maps. The GM CBF histograms

were comparable between vendors (Figure 4d). The GE WM CBF histogram had a higher mean, but had the same shape as the Philips WM CBF histogram. The wsCV histograms, on the other hand, were less comparable (Figure 5d). The spatial GM wsCV distribution of Philips had a higher mean and was wider compared to GE. This difference in mean and spread was even larger for the WM.

Discussion

The most important result of this study is that - despite several voxel-wise differences between vendors - there were no inter-vendor differences in mean CBF or wsCV on a total GM level. This can be explained by the fact that the variation between the sessions can for a large part be attributed to physiological factors, as was previously noted in single-vendor reproducibility studies [11,29–31]. For clinical studies that focus on the GM in total, it may therefore be more important to minimize and account for physiological variation than to account for inter-vendor differences in ASL implementation.

A different picture arises for smaller GM regions or for the total WM. We observed several spatial differences between vendors which can mainly be explained by differences in the readout module. The most visually striking inter-vendor difference on all CBF- and wsCV-maps was in the WM. The GM-WM CBF ratio of the 2D readout (Philips) was twice as large as the ratio of the 3D

Table 2. Inter-session statistics.

	GE	CI (n = 22)	Philips	CI (n = 22)	inter-vendor	CI (n = 44)
GM mean CBF (mL/100g/min)	65.9	48.4	65.9	42.0	65.9	45.4
GM Δ CBF	-0.4	-3.5	3.9	0.6	0.0	-2.7
GM $SD_{\Delta CBF}$	7.1	4.8	7.5	5.1	8.9	7.0
GM lower LOA	-14.3	-18.2	-10.4	-14.8	-17.5	-20.9
GM upper LOA	13.6	9.7	17.5	14.4	17.5	14.2
GM wsCV (%)	10.8	6.2	15.3	5.4	13.6	9.8
WM mean CBF (mL/100g/min)	30.5	22.0	39.0	9.1	22.9	15.6
WM Δ CBF	-0.6	-2.2	1.0	0.1	15.0	14.0
WM $SD_{\Delta CBF}$	3.6	2.4	2.1	1.4	3.5	2.7
WM lower LOA	-7.6	-9.6	-5.7	-4.3	8.3	7.0
WM upper LOA	6.4	4.4	8.3	4.1	21.8	20.5
WM wsCV (%)	11.7	9.5	13.9	12.2	15.0	13.7
GM-WM CBF ratio	2.2	1.9	2.5	3.4	2.9	2.4

Mean and Δ CBF represent the inter-session CBF mean and paired difference respectively.

The limits of agreement (LOA) represent $\Delta CBF \pm 1.96$ standard deviation of the paired difference ($SD_{\Delta CBF}$).

CI = confidence interval, CBF = cerebral blood flow, GE = General Electric, GM = gray matter,

WM = white matter, wsCV = within-subject coefficient of variation.

doi:10.1371/journal.pone.0104108.t002

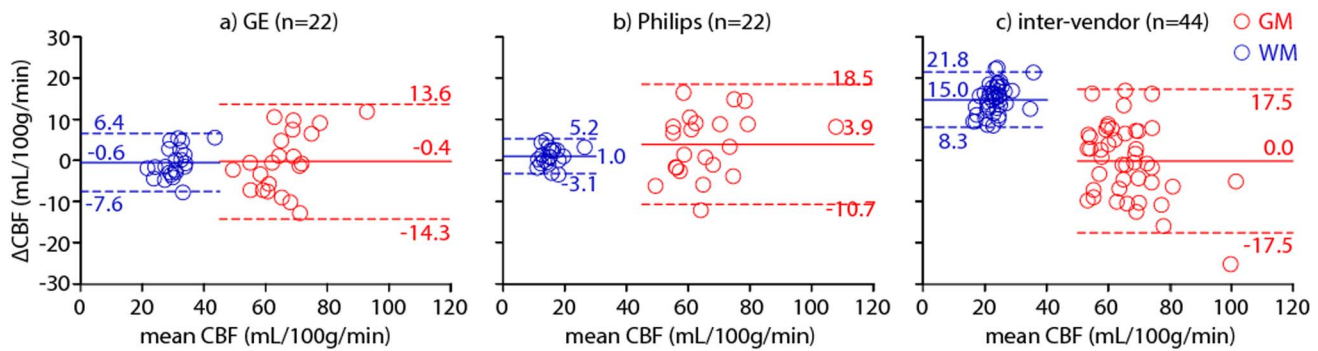


Figure 2. Bland-Altman plots. Intra-vendor a) GE (n=22) and b) Philips (n=22) and c) inter-vendor (n=44) GM (red) and WM (blue) CBF differences are plotted against mean CBF. Continuous and broken lines indicate mean difference and limits of agreement (mean difference \pm 1.96 standard deviation of the paired difference) respectively. CBF = cerebral blood flow, GM = gray matter, WM = white matter. doi:10.1371/journal.pone.0104108.g002

readout (GE), which is in agreement with a previous readout comparison on a single Siemens scanner [13]. This can be explained by the larger extent of spatial smoothing of a spiral 3D readout (GE) compared to the 2D readout (Philips), which leads to more contamination of the GM signal into the WM and vice versa.

Therefore, a 2D readout seems most suitable when the goal is to acquire uncontaminated GM or WM CBF – although the ability of ASL to measure WM CBF is debatable due to the long transit time of WM [32].

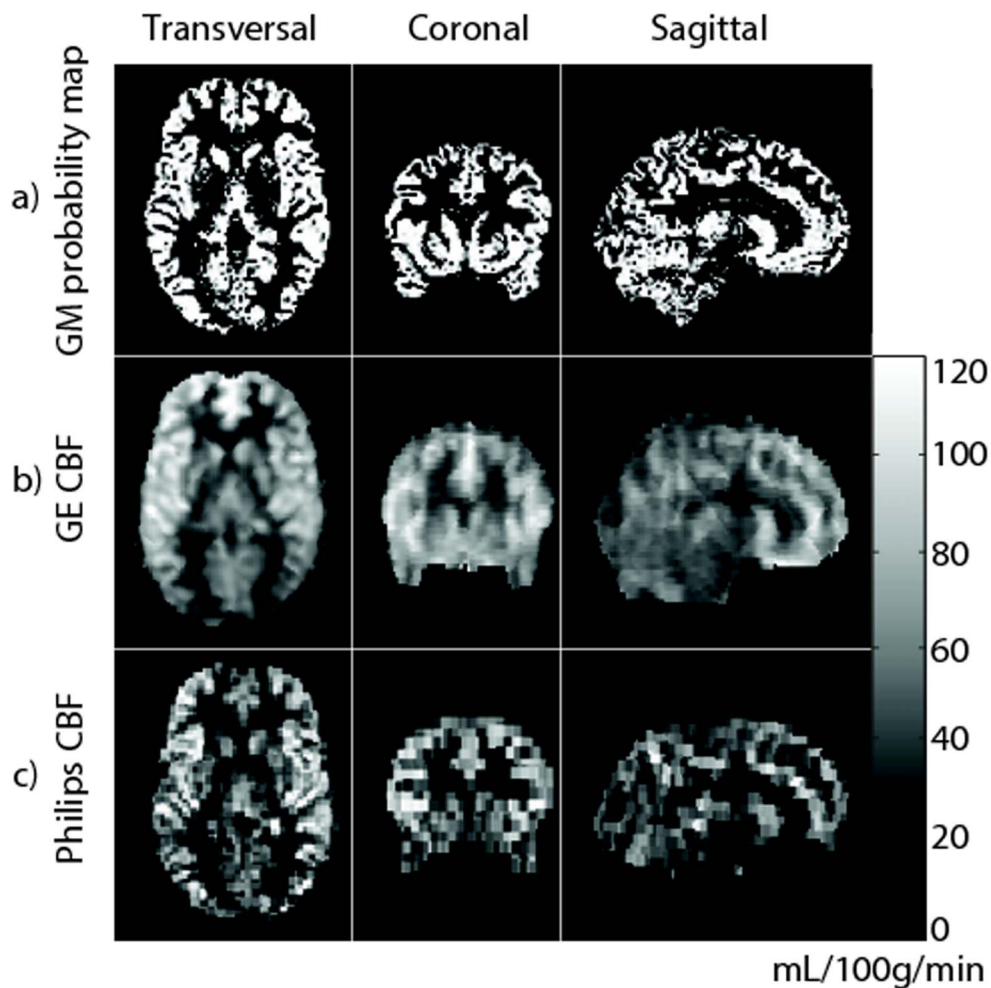


Figure 3. Cerebral blood flow maps of a representative subject of GE (b) and Philips (c), as compared to gray matter (GM) tissue probability map (a; for this example the GE 3D T1-weighted image was used). Maps are registered, re-sliced, skull-stripped and shown in native space. doi:10.1371/journal.pone.0104108.g003

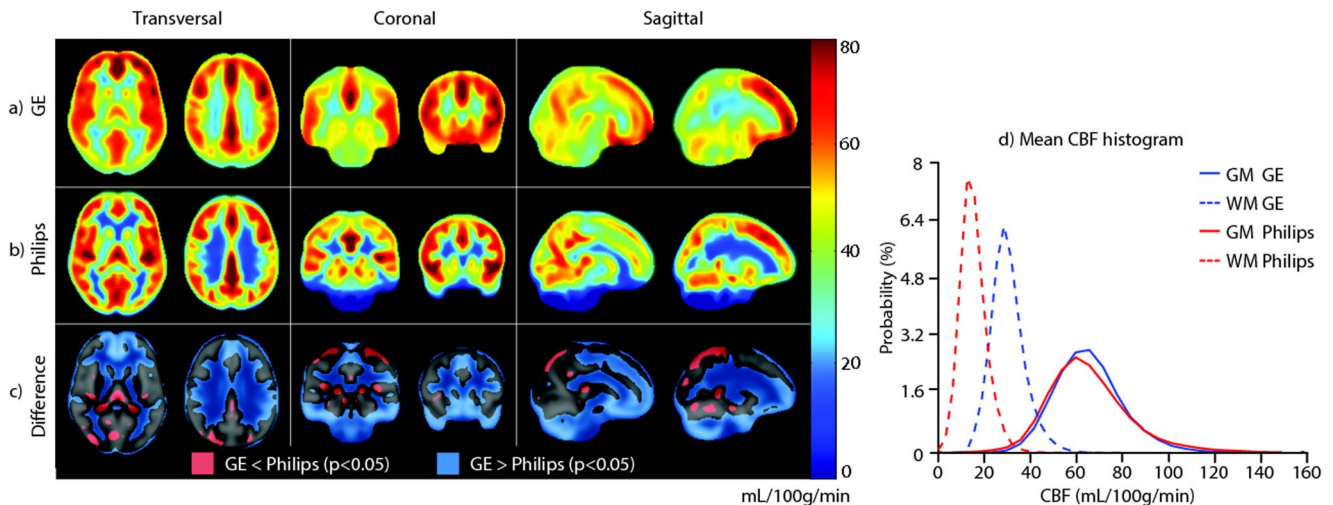


Figure 4. Mean cerebral blood flow (CBF) maps of all subjects ($n=22$) are shown for GE (a) and Philips (b), averaged for both sessions. Voxel-wise significant inter-vendor differences are visualized by a binary parametric map projected on the gray matter (GM) probability map (c). Red voxels represent where $GE < Philips$ ($p < 0.05$), blue voxels represent where $GE > Philips$ (Bonferroni corrected $p < 0.05$). On the right, mean CBF histograms are shown for the total GM and white matter (WM) (d).
doi:10.1371/journal.pone.0104108.g004

This difference in spatial smoothing may also explain the homogeneous GM appearance of the mean CBF and wsCV maps acquired with GE as compared to the more heterogeneous appearance of those acquired with Philips. In addition, it may explain the significant inter-vendor CBF difference within the subcortical GM since this area is surrounded by WM and therefore suffers more from smoothing with WM signal in GE (Figure 4c). Another explanation for the smaller spatial variation of GE, is its higher SNR compared to Philips. The SNR at GE is most probably higher because of the intrinsically high SNR of a 3D readout and because background suppression is more efficient for a single-volume readout as compared to a multi-slice readout [13]. In addition, parallel imaging was not available in the GE sequence, but was turned on in the Philips sequence. To what extent the heterogeneous appearance of the Philips CBF maps has a physiological origin or is rather the result of a too low SNR, cannot be differentiated with these data.

In regions with long arrival times - i.e. the posterior vascular territory and posterior watershed area - lower CBF and higher wsCV was observed in GE but not in Philips (Figures 4 and 5) [5]. This inter-vendor difference can be explained by differences in the effective post-labeling delay (PLD) between the readouts, even though both acquisitions had the same initial PLD (1525 ms). Whereas the 3D readout obtains all ASL signal for the total 3D volume at a single time-point - i.e. after 1525 ms PLD - the 2D readout obtains signal from each slice sequentially. With this multi-slice acquisition, each slice exhibits a longer effective PLD compared to its previous slice. This inferior-superior PLD increase of the 2D readout (Philips) allows the labeled blood more time to reach the superior slices compared to the homogeneous PLD of the 3D readout (GE). Therefore, the PLD may have been too short for the label to reach the superior slices in 3D (GE), whereas the effective PLD for the superior slices in 2D (Philips) was sufficient. These inter-vendor CBF differences and higher wsCV for GE in superior regions with long transit times are probably resolved by selecting a longer PLD for the 3D readout, such as 2000 ms [3].

Other prominent spatial inter-vendor CBF (Figure 4) and wsCV (Figure 5) differences were observed on the brain edges. We observed higher CBF and lower wsCV in anterior and inferior

regions in Philips but not in GE. The prominent inferior CBF and wsCV differences (Figure 4c and Figure 5c) are partly due to the fact that these slices were simply not acquired by the 2D readout (Philips). With a 2D sequence, it is common practice to scan cerebral slices only as well as to optimize the PLD, T1 decay and background suppression for the cerebral slices. These issues do not apply for a 3D sequence, whose 3D slab usually has whole-brain coverage. The differences in the other areas can be explained by susceptibility artifacts from bone-air transitions at the paranasal sinuses and mastoid air cells present in the gradient-echo T2*-weighted readout implemented by Philips [33]. In addition, it is expected that the echo-planar imaging readout (Philips) exhibits geometric distortion in these regions [33]. The T2-weighted spin-echo readout employed by GE is much less sensitive to these artifacts, in comparison to the gradient-echo readout employed by Philips. For these reasons, a 3D readout is superior in regions such as the orbito-frontal lobe and cerebellum compared to a 2D readout. This especially favors the use of a 3D readout for clinical applications of ASL, since pathologies in these regions could remain undetected on a 2D readout [34–36].

A limitation of the current study is that we did not acquire spatial M_0 -maps with the same readout in Philips. By employing a voxel-wise normalization of the ASL-signal, these maps would have opposed the T_2^* susceptibility effects, since these will be approximately equally large for the ΔM and M_0 -map. Therefore, Philips spatial M_{0a} -maps could have improved quantification in regions of air-tissue transitions, which may have diminished the inter-vendor variation to a certain extent. However, the added value of spatial M_0 -maps is limited since they cannot improve the lower SNR of the gradient-echo readout (Philips) near the air-tissue transitions. Therefore, the inter-vendor reproducibility in these regions is expected to remain low.

The current study may also be limited by the inter-vendor calibration of quantification parameters. These may remain arbitrary, mostly because they have been derived from simulations rather than measurements. One example is the inter-vendor differences in labeling efficiency due to a different number of background suppression pulses (5 and 2 for GE and Philips respectively) [21]. One way to deal with this is to scale to a phase-

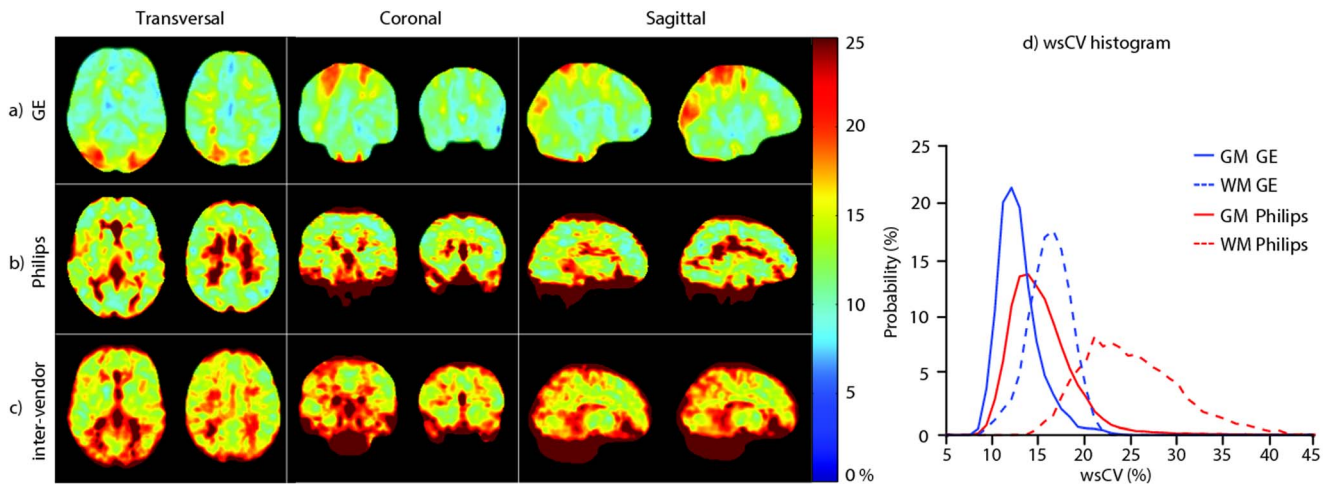


Figure 5. a) GE and b) Philips intra- and c) inter-vendor within-subject coefficient of variability (wsCV)-maps. d) wsCV histograms are shown on the right for the total gray matter (GM) and white matter (WM).
doi:10.1371/journal.pone.0104108.g005

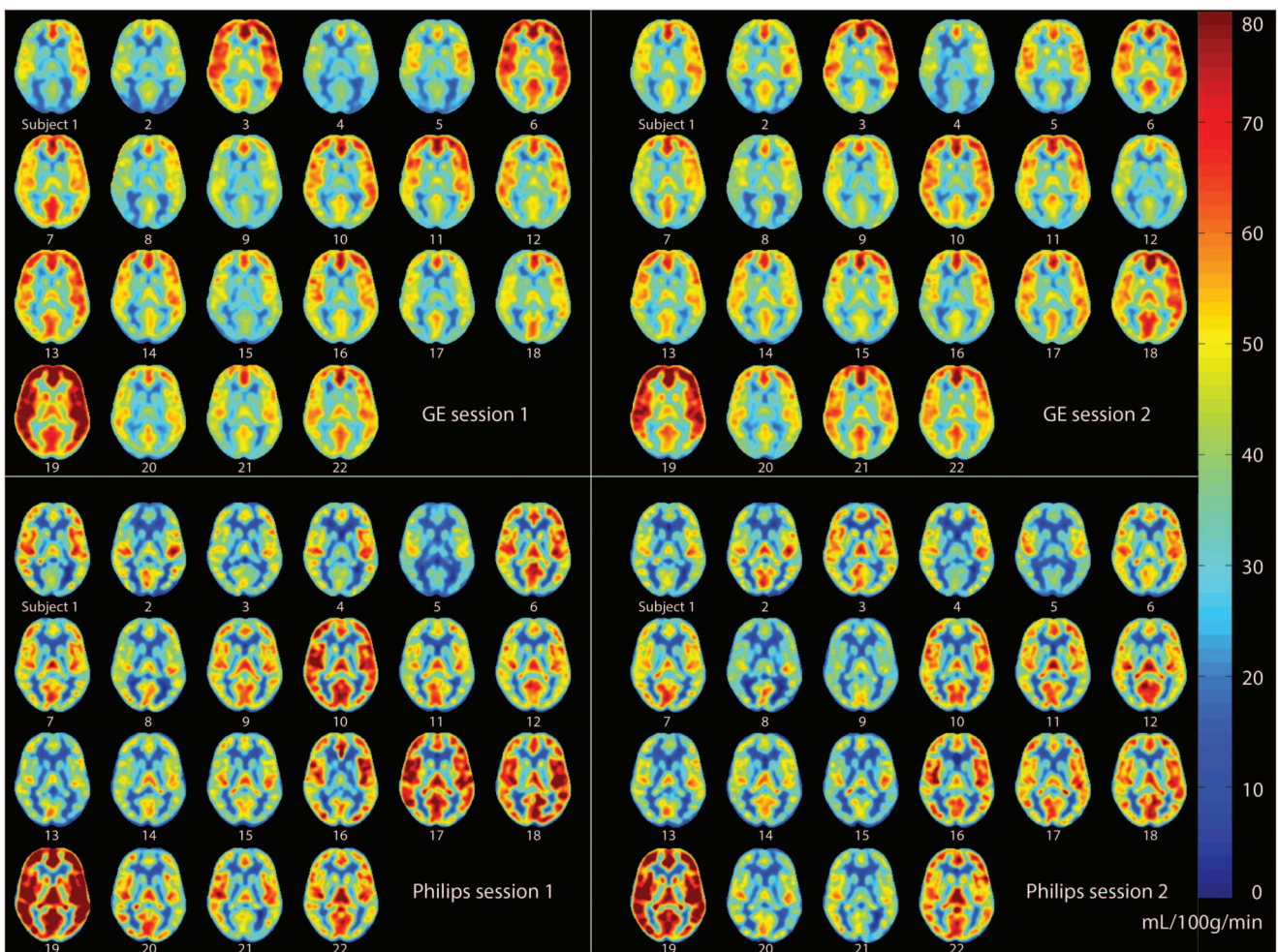


Figure 6. Single transversal cerebral blood flow slice of all subjects (n = 22) for GE (upper quadrants) and Philips (lower quadrants), session 1 (left quadrants) and session 2 (right quadrants), after spatial normalization.
doi:10.1371/journal.pone.0104108.g006

contrast MRI sequence of the main feeding arteries [20]. However, this would shift the inter-vendor CBF variation from the ASL-sequence towards the phase-contrast MRI measurements.

Inter-vendor CBF and wsCV differences were observed on a voxel-level but not on the total GM level. Apparently, the effects of the abovementioned readout differences do cancel out when sufficient GM voxels are averaged. There are several explanations for this observation. First, the higher SNR of the 3D module may be important on a voxel-level, but if sufficient GM voxels are averaged physiological variation seems to outnumber the SNR differences between the readout modules. Second, the smoothing of the GE 3D readout averages signal from multiple GM voxels which increases SNR and subsequently decreases the wsCV within a single voxel. This effect is similar to averaging signal from multiple GM voxels of the 2D readout in post-processing. Therefore, this difference of spatial signal averaging between both readouts becomes apparent on a voxel-level but is negligible when all GM voxels are averaged.

It should be acknowledged that this study evaluated healthy controls only. The abovementioned inter-vendor readout differences could become more or less important in patients, considering the different spatial CBF variation in patients compared to healthy controls. Furthermore, these inter-vendor differences should not be generalized to all MRI vendors. Visual readout differences between GE and Siemens, who both use a 3D approach, may be smaller than the readout differences in the current study [13].

References

- Golay X, Hendrikse J, Lim TC (2004) Perfusion imaging using arterial spin labeling. *Top Magn Reson Imaging* 15: 10–27. 00002142-200402000-00003 [pii].
- Williams DS, Detre JA, Leigh JS, Koretsky AP (1992) Magnetic resonance imaging of perfusion using spin inversion of arterial water. *Proc Natl Acad Sci U S A* 89: 212–216.
- Alsop DC, Detre JA, Golay X, Gunther M, Hendrikse J et al. (2014) Recommended implementation of arterial spin-labeled perfusion MRI for clinical applications: A consensus of the ISMRM perfusion study group and the European consortium for ASL in dementia. *Magn Reson Med*. 10.1002/mrm.25197 [doi].
- Chen Y, Wolk DA, Reddin JS, Korczykowski M, Martinez PM et al. (2011) Voxel-level comparison of arterial spin-labeled perfusion MRI and FDG-PET in Alzheimer disease. *Neurology* 77: 1977–1985. WNL0b013c31823a0ef7 [pii];10.1212/WNL.0b013c31823a0ef7 [doi].
- Petersen ET, Mouridsen K, Golay X (2010) The QUASAR reproducibility study, Part II: Results from a multi-center Arterial Spin Labeling test-retest study. *Neuroimage* 49: 104–113. S1053-8119(09)00859-3 [pii];10.1016/j.neuroimage.2009.07.068 [doi].
- Xu G, Rowley HA, Wu G, Alsop DC, Shankaranarayanan A et al. (2010) Reliability and precision of pseudo-continuous arterial spin labeling perfusion MRI on 3.0 T and comparison with 15O-water PET in elderly subjects at risk for Alzheimer's disease. *NMR Biomed* 23: 286–293. 10.1002/nbm.1462 [doi].
- Jahng GH, Song E, Zhu XP, Matson GB, Weiner MW et al. (2005) Human brain: reliability and reproducibility of pulsed arterial spin-labeling perfusion MR imaging. *Radiology* 234: 909–916. 234/3/909 [pii];10.1148/radiol.2343031499 [doi].
- Detre JA, Rao H, Wang DJ, Chen YF, Wang Z (2012) Applications of arterial spin labeled MRI in the brain. *J Magn Reson Imaging* 35: 1026–1037. 10.1002/jmri.23581 [doi].
- Hendrikse J, Petersen ET, Golay X (2012) Vascular disorders: insights from arterial spin labeling. *Neuroimaging Clin N Am* 22: 259–2xi. S1052-5149(12)00005-6 [pii];10.1016/j.nic.2012.02.003 [doi].
- Golay X (2009) How to do an ASL multicenter neuroimaging study. *Proc Intl Soc Mag Reson Med* 17.
- Liu T, Wierenga C, Mueller B, F-BIRN (2008) Reliability and Reproducibility of Arterial Spin Labeling Perfusion Measures Assessed with a Multi-Center Study. *Proc Intl Soc Mag Reson Med* 16: 3338.
- Kilroy E, Apostolova L, Liu C, Yan L, Ringman J et al. (2013) Reliability of two-dimensional and three-dimensional pseudo-continuous arterial spin labeling perfusion MRI in elderly populations: Comparison with 15o-water positron emission tomography. *J Magn Reson Imaging*. 10.1002/jmri.24246 [doi].
- Vidorreta M, Wang Z, Rodriguez I, Pastor MA, Detre JA et al. (2012) Comparison of 2D and 3D single-shot ASL perfusion fMRI sequences. *Neuroimage* 66C: 662–671. S1053-8119(12)01091-9 [pii];10.1016/j.neuroimage.2012.10.087 [doi].
- Chen Y, Wang DJ, Detre JA (2011) Test-retest reliability of arterial spin labeling with common labeling strategies. *J Magn Reson Imaging* 33: 940–949. 10.1002/jmri.22345 [doi].
- Binnewijzend MA, Kuijter JP, Benedictus MR, van der Flier WM, Wink AM et al. (2013) Cerebral blood flow measured with 3D pseudocontinuous arterial spin-labeling MR imaging in Alzheimer disease and mild cognitive impairment: a marker for disease severity. *Radiology* 267: 221–230. radiol.12120928 [pii];10.1148/radiol.12120928 [doi].
- Donahue MJ, Ayad M, Moore R, van OM, Singer R et al. (2013) Relationships between hypercarbic reactivity, cerebral blood flow, and arterial circulation times in patients with moyamoya disease. *J Magn Reson Imaging*. 10.1002/jmri.24070 [doi].
- Alsop DC, Detre JA (1996) Reduced transit-time sensitivity in noninvasive magnetic resonance imaging of human cerebral blood flow. *J Cereb Blood Flow Metab* 16: 1236–1249. 10.1097/00004647-199611000-00019 [doi].
- St Lawrence KS, Wang J (2005) Effects of the apparent transverse relaxation time on cerebral blood flow measurements obtained by arterial spin labeling. *Magn Reson Med* 53: 425–433. 10.1002/mrm.20364 [doi].
- Lu H, Clingman C, Golay X, van Zijl PC (2004) Determining the longitudinal relaxation time (T1) of blood at 3.0 Tesla. *Magn Reson Med* 52: 679–682. 10.1002/mrm.20178 [doi].
- Aslan S, Xu F, Wang PL, Uh J, Yezhovath US et al. (2010) Estimation of labeling efficiency in pseudocontinuous arterial spin labeling. *Magn Reson Med* 63: 765–771. 10.1002/mrm.22245 [doi].
- Garcia DM, Duhamel G, Alsop DC (2005) Efficiency of inversion pulses for background suppressed arterial spin labeling. *Magn Reson Med* 54: 366–372. 10.1002/mrm.20556 [doi].
- Lu H, Nagae-Poetscher LM, Golay X, Lin D, Pomper M et al. (2005) Routine clinical brain MRI sequences for use at 3.0 Tesla. *J Magn Reson Imaging* 22: 13–22. 10.1002/jmri.20356 [doi].
- Herscovitch P, Raichle ME (1985) What is the correct value for the brain-blood partition coefficient for water? *J Cereb Blood Flow Metab* 5: 65–69. 10.1038/jcbfm.1985.9 [doi].
- Heijtel DF, Mutsaerts HJ, Bakker E, Schober P, Stevens MF et al. (2014) Accuracy and precision of pseudo-continuous arterial spin labeling perfusion during baseline and hypercapnia: a head-to-head comparison with O HO positron emission tomography. *Neuroimage*. S1053-8119(14)00102-5 [pii];10.1016/j.neuroimage.2014.02.011 [doi].
- Chalela JA, Alsop DC, Gonzalez-Atavales JB, Maldjian JA, Kasner SE et al. (2000) Magnetic resonance perfusion imaging in acute ischemic stroke using continuous arterial spin labeling. *Stroke* 31: 680–687.

In conclusion, the current study shows that pCASL results do not differ between vendors on a total GM level. Therefore, the reliability of averaged CBF-values for the total GM can be expected to be equal in single- and multi-vendor studies. However, the reliability of measurements in GM regions or in the WM, is impeded by differences between the readout modules of both vendors. Therefore, our results strongly encourage the standardization of ASL implementations among vendors, which was also advocated by the recent ASL consensus paper [3].

Acknowledgments

The authors are grateful to S. van Bekkum, BSc, P.F.C. Groot, MSc, G.C. Houston, PhD and C.P. Mendez-Orellana, MSc for assistance with data collection, to E.E. Bron, MSc for help with data post-processing, and to I. Groote, MD PhD and S. Wastling, PhD for help with the manuscript. The authors wish to express their gratitude to the contribution of the COST-AID Action BM1103 (European Cooperation in Science and Technology-Arterial spin labeling Initiative in Dementia). This manuscript has been presented and discussed multiple times at international meetings of this Action.

Author Contributions

Conceived and designed the experiments: HJMMM DFRH JPAK MJPvO CBLMM MS AJN. Performed the experiments: HJMMM RMES DFRH JPAK MS. Analyzed the data: HJMMM RMES JPAK MJPvO CBLMM MS AJN. Contributed reagents/materials/analysis tools: HJMMM RMES JPAK MJPvO CBLMM MS AJN. Wrote the paper: HJMMM RMES DFRH MJPvO CBLMM MS AJN.

26. Ashburner J (2007) A fast diffeomorphic image registration algorithm. *Neuroimage* 38: 95–113. S1053-8119(07)00584-8 [pii];10.1016/j.neuroimage.2007.07.007 [doi].
27. Levene Howard, Olkin I, and Hotelling H (1960) *Contributions to Probability and Statistics: Essays in Honor of Harold Hotelling*. Stanford University Press. 292 p.
28. Bland JM, Altman DG (1999) Measuring agreement in method comparison studies. *Stat Methods Med Res* 8: 135–160.
29. Floyd TF, Ratcliffe SJ, Wang J, Resch B, Detre JA (2003) Precision of the CASL-perfusion MRI technique for the measurement of cerebral blood flow in whole brain and vascular territories. *J Magn Reson Imaging* 18: 649–655. 10.1002/jmri.10416 [doi].
30. Parkes LM, Rashid W, Chard DT, Tofts PS (2004) Normal cerebral perfusion measurements using arterial spin labeling: reproducibility, stability, and age and gender effects. *Magn Reson Med* 51: 736–743. 10.1002/mrm.20023 [doi].
31. Gevers S, van Osch MJ, Bokkers RP, Kies DA, Teeuwisse WM et al. (2011) Intra- and multicenter reproducibility of pulsed, continuous and pseudo-continuous arterial spin labeling methods for measuring cerebral perfusion. *J Cereb Blood Flow Metab* 31: 1706–1715. jcbfm201110 [pii];10.1038/jcbfm.2011.10 [doi].
32. van Gelderen P, de Zwart JA, Duyn JH (2008) Pitfalls of MRI measurement of white matter perfusion based on arterial spin labeling. *Magn Reson Med* 59: 788–795. 10.1002/mrm.21515 [doi].
33. Deichmann R, Josephs O, Hutton C, Corfield DR, Turner R (2002) Compensation of susceptibility-induced BOLD sensitivity losses in echo-planar fMRI imaging. *Neuroimage* 15: 120–135. 10.1006/nimg.2001.0985 [doi];S1053811901909851 [pii].
34. Timmann D, Konczak J, Ilg W, Donchin O, Hermsdörfer J et al. (2009) Current advances in lesion-symptom mapping of the human cerebellum. *Neuroscience* 162: 836–851. S0306-4522(09)00095-5 [pii];10.1016/j.neuroscience.2009.01.040 [doi].
35. Wolf RC, Thomann PA, Sambataro F, Vasic N, Schmid M et al. (2012) Orbitofrontal cortex and impulsivity in borderline personality disorder: an MRI study of baseline brain perfusion. *Eur Arch Psychiatry Clin Neurosci* 262: 677–685. 10.1007/s00406-012-0303-1 [doi].
36. Walther S, Federspiel A, Horn H, Razavi N, Wiest R et al. (2011) Resting state cerebral blood flow and objective motor activity reveal basal ganglia dysfunction in schizophrenia. *Psychiatry Res* 192: 117–124. S0925-4927(10)00424-5 [pii];10.1016/j.psychres.2010.12.002 [doi].